

## STOKES PARAMETERS FOR OH SOURCES

W. A. COLES AND V. H. RUMSEY

Department of Applied Physics and Information Science, University of California, San Diego

*Received 1969 March 3; revised 1969 June 23*

### ABSTRACT

Stokes parameters for certain of the 1665- and 1667-MHz OH emission lines of the sources in W3, W22, W24B2, W33, W43, W49, Ori A, Cas A, and NGC 6334; and for the 1612- and 1720-MHz lines of W28, G5.9-04, W43, W44, and W51 were measured during 1968 February and May. At 1665 MHz but not at 1667 MHz, W33 showed strong time variation from February to May and during a 10-day period in May. There is evidence of time variability in W3 at 1665 MHz. Emission at 1667 MHz from a dark cloud at  $l = 168^{\circ}74$ ,  $b = -15^{\circ}50$  showed less than 10 percent polarization. No polarization was detected in any absorption feature, within an accuracy depending on the source strength: 2 percent accuracy for Cassiopeia is typical.

### I. INTRODUCTION

Spectra of the four ground-state OH transitions (at 1612, 1665, 1667, and 1720 MHz) are remarkably complex for almost all the sources that have been observed. An increase of resolution in space, in time, or in polarization has invariably revealed a wealth of new detail about the structure of the OH sources. Measurements of polarization, notably those by Palmer and Zuckerman (1967) and by Ball and Meeks (1968), have shown that many features of the spectra have a high degree of circular polarization, and the sense of polarization often varies rapidly from one feature to another. Strong indications of time variations have also been noted.

The measurements to be described in this paper were made with a specially designed polarimeter that was installed in the 85-foot reflector at Hat Creek. Table 1 lists the sources that were observed. As a check, several that had been previously measured were included in the list, but for most sources this work constitutes the first measurement of Stokes parameters. The observations were directed particularly to sources that were known to emit strongly in the satellite lines at 1612 and 1720 MHz.

### II. OBSERVATIONS

The observations take the form of spectra of the Stokes parameters  $S_0$ ,  $S_1$ ,  $S_2$ , and  $S_3$ . They are defined as follows. If  $T(\Phi)$  is the antenna temperature for linear polarization at a position angle  $\Phi$ , and if  $T(R)$  and  $T(L)$  are the temperatures for right- and left-circular polarization, defined with respect to the direction of propagation, then

$$\begin{aligned} S_0 &= T(\Phi) + T(\Phi + 90^\circ), \quad \text{for any angle } \Phi, \\ &= T(R) + T(L), \end{aligned}$$

$$S_1 = T(0^\circ) - T(90^\circ), \quad S_2 = T(45^\circ) - T(135^\circ), \quad S_3 = T(R) - T(L).$$

The format of the results is illustrated by Figure 1. The abscissa for the spectra is the Doppler velocity calculated with respect to the rest frequencies adopted by Goss (1958), namely, 1612.231, 1665.401, 1667.358, and 1712.533 MHz. The scale of the ordinate is antenna temperature. For a point source,  $1^\circ$  K corresponds to  $5.8 \pm 5$  f.u.

The OH source in the H II region W3 (IC 1795) has been the subject of several previous investigations. We observed it partly as a check on our apparatus and partly to look for time variations. Our results for February and May periods are self-consistent and

TABLE 1  
OH SOURCES OBSERVED 1968 FEBRUARY AND MAY

SOURCE	$l$	$b$	FREQUENCY (MHz)			
			1612	1665	1667	1720
W3.....	133.95	+ 1.01	...	E	...	...
W22.....	353.15	+ 0.69	...	...	A	...
W24B2.....	0.67	- 0.08	...	E	...	...
W28.....	6.58	- 0.19	...	...	...	E
G5.9-0.4*.....	5.88	- 0.37	E	...	...	...
W33.....	12.65	- 0.04	...	A, E	A, E	...
W43.....	30.78	- 0.14	E	A, E	A, E	...
W44.....	34.65	- 0.44	A	...	...	E
W49.....	43.17	- 0.01	...	E	...	...
W51.....	49.17	- 0.38	A, E	...	...	E
Ori A.....	209.01	-19.38	...	E	...	...
Cas A.....	111.74	- 2.14	...	...	A	...
NGC 6334.....	351.24	+ 0.77	...	A, E	...	...
S110†.....	168.74	-15.50	...	...	E	...

NOTE.—A = absorption; E = emission.

\* New source near W28.

† Dark cloud observed by Heiles (1968).

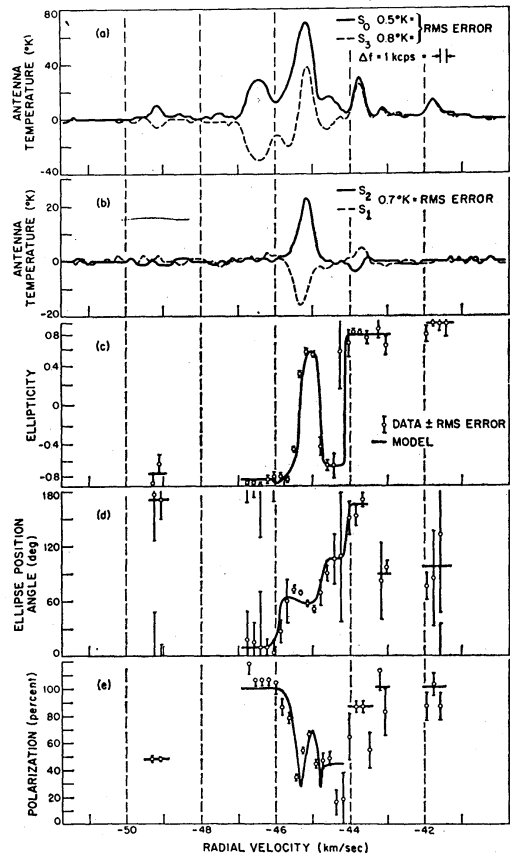
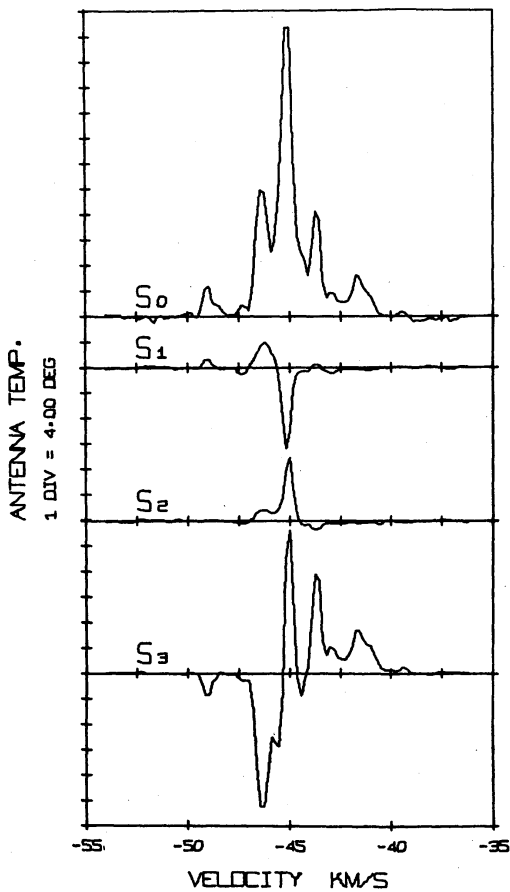


FIG. 1.—Source W3 at 1665 MHz. *Left*, our spectra taken during 1968 May; *right*, spectra of Meeks *et al.* (1966) taken during 1965 November.

show small but significant differences from previous observations. Figure 1 shows the comparison of the results of Meeks *et al.* (1966) with ours. The difference, which shows up mainly in  $S_1$  and  $S_2$ , does not seem to be caused by any identifiable difference of experimental conditions, such as a simple pointing error.

OH emission from the source W33 was first detected by Goss (1968), who used a linearly polarized antenna. The identification of this source is in doubt, and there is ambiguity about its distance: the near and far points are estimated at 4.7 and 14.8 kpc. The  $158\alpha$  line at  $+38.6$  km sec $^{-1}$  agrees well with the OH emission line (Dieter 1967). Our results are shown in Figure 2. It will be seen that there is clear correspondence between the features at 1665 and 1667 MHz, in both velocity and polarization. Comparison of the 1665-MHz results taken in February and May 11–14 shows a striking difference, especially in  $S_2$ . This prompted a third look at W33 on May 24. It will be seen from Figure 2 that some prominent features in  $S_0$  and  $S_2$  changed considerably, or even disappeared, in the 10-day interval between May 14 and May 24. The interpretation of these remarkable results has been discussed previously (Coles, Rumsey, and Welch 1968), and the subject of time variations is considered separately later on. Broadly speaking, this source appears to be similar to the time-varying OH source NGC 6334, except that its intrinsic strength is 10 times greater if the distance is taken as 4.7 kpc or 80 times greater if the distance is taken as 14.8 kpc.

The remaining observations are summarized in Table 2. All of the sources are galactic, and they include H II regions and nonthermal sources. Many samples of each spectrum were taken, and the results presented here were obtained by using the analysis procedure described in § VI. In most cases it was possible to fit the prominent features of a spectrum to Gaussian profiles, and so to arrive at a velocity, line width, and temperature for any particular feature. When a feature shows clearly in  $S_0$ ,  $S_1$ ,  $S_2$ , and  $S_3$ , all four spectra are employed in fitting to the Gaussian model. Otherwise, the results given in Table 2 are derived from the  $S_0$  spectrum alone, as in the cases of W28 and W43.

The source W22 (NGC 6357) appears to be a complex of three thermal sources. It has been examined in the continuum by Mezger and Henderson (1967) and by Goss (1968). Goss has discussed it in detail and presents spectra with 2-kHz resolution for all four OH transitions. Our spectra for the 1667-MHz line agree very well with those of Goss. We found no evidence of polarization, with upper bounds of 6 and 2.5 percent in the degree of polarization for the two strongest features.

W28 is a complex source that involves at least three components, one of which is M20. Most of the flux comes from a nonthermal source believed to be a supernova remnant. The disagreement between the kinematic distance and the photometric distance to M20 suggests a large peculiar motion. Goss has adopted a distance of 2.0 kpc to the OH source, but a peculiar motion similar to that of M20 could cause a large error in this figure. The OH does not appear to be associated with the thermal source, and the closest reported H I absorption velocity is  $+7.5$  km sec $^{-1}$  (Goss 1968). Strong OH emission is found at 1720 MHz, but weak absorption in the other three lines. We observed the 1720-MHz transition during both the February and May periods. The spectra for May are shown in Figure 3. Polarization measurements have recently been made by Ball and Staelin (1968) and Turner (1968). Our results agree well with those of Turner, but Ball and Staelin present only the  $S_0$  spectrum. Turner has mapped the source by using the 140-foot antenna of the NRAO and finds the emission features to be spatially separated, and distinct from the position of maximum absorption. Our spectra show two broad, unpolarized features, and two stronger and narrower features with slight circular polarization. The strong features appeared to be about 10 percent weaker in May than in February. We have no way of checking whether this is an intrinsic variation of the source, and we have no reason to suspect an instrumental effect. The  $S_3$  spectrum indicates a complexity not apparent in the  $S_0$  spectrum, perhaps showing that each of the two narrow features is double.

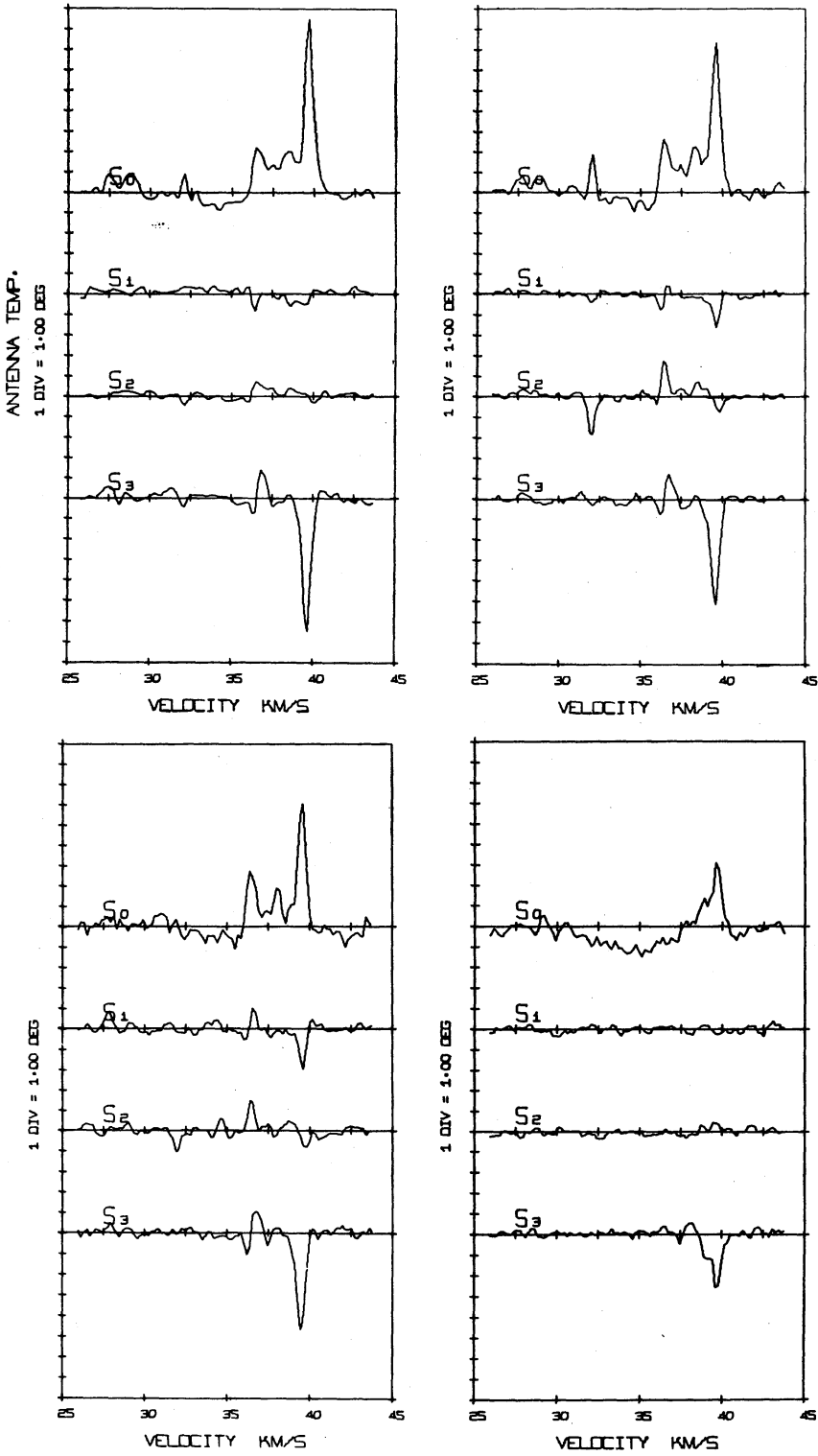


FIG. 2.—Main-line spectra of W33 illustrating its variation with time. Measurements at 1665 MHz were taken February 15, 16, and 18 (*upper left*); May 11–14 (*upper right*), and May 24 (*lower left*). The 1667-MHz spectra were taken May 11–14 (*lower right*).

Table 2  
Summary of the Source Parameters

Source	Trans. Freq. MHz	Radial Velocity V, km/s	Half Power Width, KHz	Peak Temperatures <sup>o</sup> K				Degree of Poln. %	Axial Ratio	Posn Angle	Class	
				S <sub>0</sub>	S <sub>1</sub>	S <sub>2</sub>	S <sub>3</sub>					
W3	1665.	- see Coles, Rumsey, and Welch (1968).									c	
W22	1667.	-4.0 ± 0.4	39.3 ± 2.0	-1.76 ± 0.13	-0.07	0.07	0.01	< 6			a	
		-1.36 .1	7.8 1.4	-.94 .23	.11	-.26	.04	< 29			a	
		+5.58 .02	7.9 .3	-5.61 .23	.09	-.09	.05	< 2.4			a	
		+7.56 .02	5.7 .3	-1.58 .14	-.07	-.23	.28	< 23			a	
W24B2 W28	1665. 1720.	- no model fitted to observations -									c	
		+5.61 ± 0.2	16.47 ± 1.5	2.21 ± .2							d	
		+9.30 .02	7.54 .3	8.73 .4							d	
		+10.79 .02	5.45 .3	14.05 .6							d	
G5.9-0.4 W33	1612.	+12.54 .2	29.31 1.5	2.60 .2							d	
	1665. 1667.	-20.60 ± .01	5.58 ± .1	23.75 ± .6							d	
W43	1665.	- see Coles, Rumsey, and Welch (1968).										
		35.32 ± 0.12	35.0 ± 1.9	-1.15 ± 0.1	.00	-.07	-.04	< 8	.29	134 <sup>o</sup>	a	
		36.29 .1	4.67 0.2	.49 .2	.13	-.04	.26	62	.60	9 <sup>o</sup>	c	
		37.93 .1	4.34 1.0	1.10 .3	-.17	-.17	.50	39	.54	112 <sup>o</sup>	c	
		38.87 .07	3.14 0.6	1.72 .8	.24	.25	-1.02	50	.66	23 <sup>o</sup>	c	
		39.68 .02	3.75 0.16	3.25 .2	-.23	.42	-2.61	79	.83	59 <sup>o</sup>	c	
		82.44 ± 0.4	23.0 ± 2.5	-0.60 ± 0.02								a
		86.25 .2	3.0 1.0	0.9 .2								c
		88.02 .2	4.0 1.0	1.0 .1								c
		90.99 .2	3.8 0.5	1.9 .07								c
	1667.	92.14 .4	42.0 2.5	-1.5 .05								c
		97.25 .2	5.0 0.6	0.5 .2								c
		98.78 .2	4.2 1.0	0.2 .1								c
		100.81 .2	3.7 1.0	0.85 .1								c
		102.61 .2	3.6 1.0	0.55 .1								c
		104.07 .2	3.7 1.0	0.45 .1								c
		81.39 ± 0.4	35.6 ± 2.5	-1.24 ± .04								a
		86.16 .2	2.9 1.0	.93 .2								c
		87.41 .2	2.6 1.0	1.15 .2								c
		90.83 .2	3.4 1.0	2.70 .2								c
1612.	92.79 .4	46.1 2.5	-2.72 .04								a	
	96.37 .2	3.8 1.0	.83 .2								c	
	27.41 ± 0.1	7.72 ± 1.0	1.9 ± 0.3								d	
	40.36 ± 0.02	6.55 ± 0.1	7.1 ± 0.3								d	
W44	1612.	43.1 ± 0.1	16.0 ± 2.0	0.63 ± 0.1							d	
		+42.0 ± 0.24	54.6 ± 3.0	-0.96 ± 0.07	-.05	-.02	.02	< 7			e	
	1720.	+42.0 .45	39.4 6.0	+66 .13	.06	-.01	.11	< 19			e	
		43.80 .04	10.4 .5	3.54 .22	.15	-.10	-.08	< 6			d	
W49 W51	1665.	- no model fitted to observations									c	
		5.17 ± 0.07	6.08 ± 0.87	-1.44 ± 0.27	.14	-.11	.05	< 13			e	
	1612.	6.85 .06	5.14 .70	-.85 .18	.05	.06	.26	< 31			e	
		59.16 .02	3.37 .3	3.0 .35	.58	.00	2.17	75	.77	0 <sup>o</sup>	c	
1720.	61.1 .2	34.9 2.2	-1.3 .1	-.02	-.08	-.01	< 7			e		
	4.71 .07	6.6 1.0	+1.1 .1	.03	.09	-.04	< 10			e		
	57.65 .15	2.0 1.8	1.2 1.0	(feature exists but parameters not meaningful)						c		
	58.3 .3	47.8 4.0	1.18 .12	.08	.03	-.10	< 11			e		
ORI A CAS A	1665.	58.52 .04	4.6 .56	2.1 .3	.79	.23	2.01	104	.67	8 <sup>o</sup>	c	
	1667.	- no model fitted to observations									c	
NGC6334 S110	1665.	1.60 ± 0.01	4.07 ± 0.15	-10.5 ± 0.5	.10	.24	-.21	< 3.1			a	
	1667.	-.25 .01	6.18 .11	-11.0 .2	-.01	.12	-.15	< 1.8			a	
		- no model fitted to observations									c	
		7.3 ± .3	5.2 ± .9	1.15 ± .26	-.06	.00	.06	< 7.4			b	

The source G5.9-0.4 is about  $1^\circ$  south of W28 and coincides with a continuum peak in this complex region. OH emission was discovered by Weaver (1968) in a survey of the region with 30-kHz resolution. The emission at 1612 MHz is very strong and appears to be uncorrelated with weaker emission in the main lines. The velocity of the 1612-MHz line,  $-21 \text{ km sec}^{-1}$ , is an impossible circular velocity for this longitude. Hence the source is probably nearby, and must have a peculiar motion greater than  $21 \text{ km sec}^{-1}$ . We examined only this 1612-MHz emission, and the spectra are shown in Figure 4. Turner (1968) has recently observed this source and finds numerous polarized features in the main lines. The  $S_0$  spectra show a single strong feature with a weaker feature blended in its low-velocity wing. However, the  $S_3$  spectrum shows a very complex structure with four circularly polarized components. Because we did not know the source

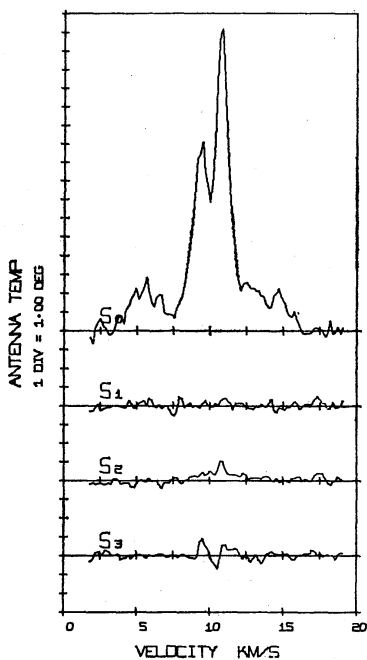


FIG. 3

FIG. 3.—Source W28 at 1720 MHz, 1968 May.

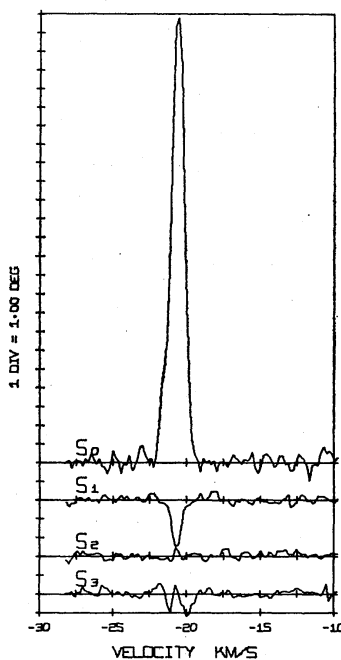


FIG. 4

FIG. 4.—Source G5.9-0.4 at 1612 MHz, 1968 May 25.

position accurately, some of the apparent linear polarization shown in the  $S_1$  spectrum may be due to the off-axis instrumental bias. For circular polarization this bias is negligible, and so the  $S_3$  spectrum is reliable.

W43 is a large and thoroughly studied H II region in the  $l = 32^\circ$  spiral arm at a distance of 7.5 kpc. The  $158\alpha$  recombination line spectrum shows a line at  $+97 \text{ km sec}^{-1}$  for this region. It also indicates the presence of a smaller H II region at  $+44 \text{ km sec}^{-1}$ , which is in the Sagittarius arm at a distance of 14.0 kpc. The first OH observations show a complex of main-line absorption features near  $+90 \text{ km sec}^{-1}$ , and a very strong emission at 1612 MHz near  $+40 \text{ km sec}^{-1}$  (Goss 1968). The 1612-MHz feature has no counterpart at 1720 MHz and shows only weakly in the main lines.

We examined the main lines near  $+90 \text{ km sec}^{-1}$ , and our spectra are shown in Figure 5. It is apparent that the complex absorption in Goss's spectra with 10-kHz resolution consist of two broad lines with many small sharp emission features superimposed. The strongest line is 8 times stronger than NGC 6334, if it is associated with the 7.5-kpc H II region. There is good agreement between the 1665- and 1667-MHz spectra for the

absorption lines and the three obvious emission features, but the weak features above  $+95 \text{ km sec}^{-1}$  do not correspond at all. The feature at  $+91 \text{ km sec}^{-1}$  fits a Zeeman splitting in a field of about  $5 \times 10^{-4}$  gauss. The two features at  $+86$  and  $+87.5 \text{ km sec}^{-1}$  have a rather complex structure with different polarizations at 1665 and 1667 MHz.

Our observations of the emission at 1612 MHz near  $+40 \text{ km sec}^{-1}$  during both February and May are shown in Figure 6. The  $+41 \text{ km sec}^{-1}$  feature is typical of strong satellite-line emission. It is weakly polarized, and the  $S_3$  spectrum shows multiple splitting. The emission source may be near the 14.0-kpc H II region because the velocity agreement is very good. Its intrinsic strength is about 20 times that of the 1720-MHz line in W28 if the distance of 2.0 kpc used by Goss for W28 is adopted. There is a striking similarity between this feature and the satellite emission in W28 and G5.9-0.4.

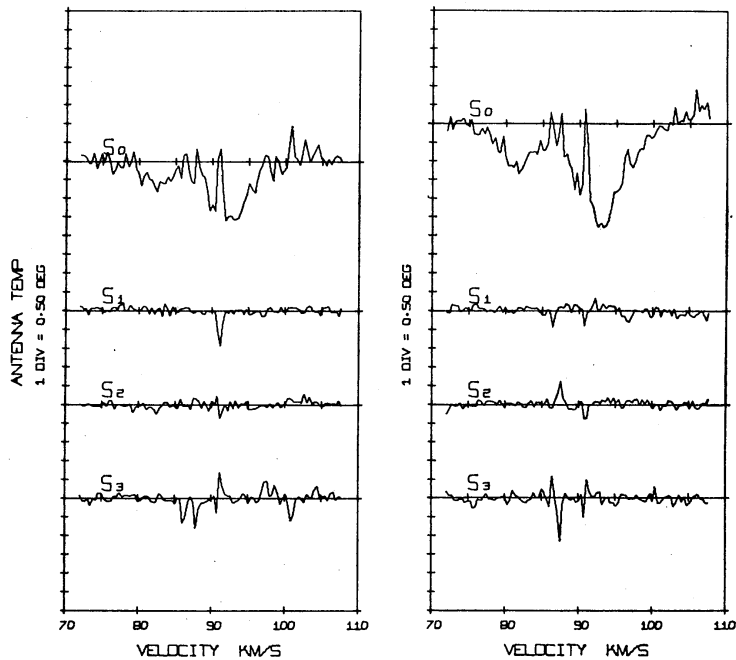


FIG. 5.—Main-line spectra of W43 at 1665 MHz during May 1968 (*left*), and at 1667 MHz during 1968 February (*right*).

The continuum source W44 consists of a nonthermal source and an H II region (Hollinger and Hobbs 1966). At 18 cm most of the flux is from the nonthermal source, which is probably a supernova remnant situated in the Sagittarius arm about 3 kpc from the Sun (Goss 1968). The satellite lines are alternately in absorption and emission as shown in Figure 7. The broad emission feature at 1720 MHz and the absorption at 1612 MHz agree well. The sharper emission features, which show no polarization in these measurements, appear to be due to a different mechanism from that causing the broad feature.

W49 has been thoroughly observed, most recently by Ball and Meeks (1968). Our spectra shown in Figure 8 have lower resolution but agree well with theirs. We find some small linear polarization, of the order of 5 percent, which is below their noise level.

The W51 region is a complex of small thermal and nonthermal sources on a weak background. The two brightest thermal sources have been resolved by Mezger and Höglund (1967) in the  $109\alpha$  line. The OH emission near  $+60 \text{ km sec}^{-1}$  appears to be associated with the brighter of these, which has a velocity of  $+59.1 \text{ km sec}^{-1}$ . A kinematic distance of 6.5 kpc has been adopted by both Mezger and Höglund (1967) and Dieter (1967). H I absorption is reported (Goss 1968) at  $+6$ ,  $+48$ , and  $+61 \text{ km sec}^{-1}$ .

There is another OH feature near  $+5 \text{ km sec}^{-1}$  which is probably in the H I cloud. OH observations were first made by Goss, the  $+60 \text{ km sec}^{-1}$  region was examined with higher resolution by Weaver, Dieter, and Williams (1968), and polarization measurements were made at 1665 MHz by Ball and Meeks (1968).

Our results are shown in Figures 9 and 10. The absorption-emission features are broad and unpolarized at both  $+60$  and  $+5 \text{ km sec}^{-1}$ , as are very similar features in W44.

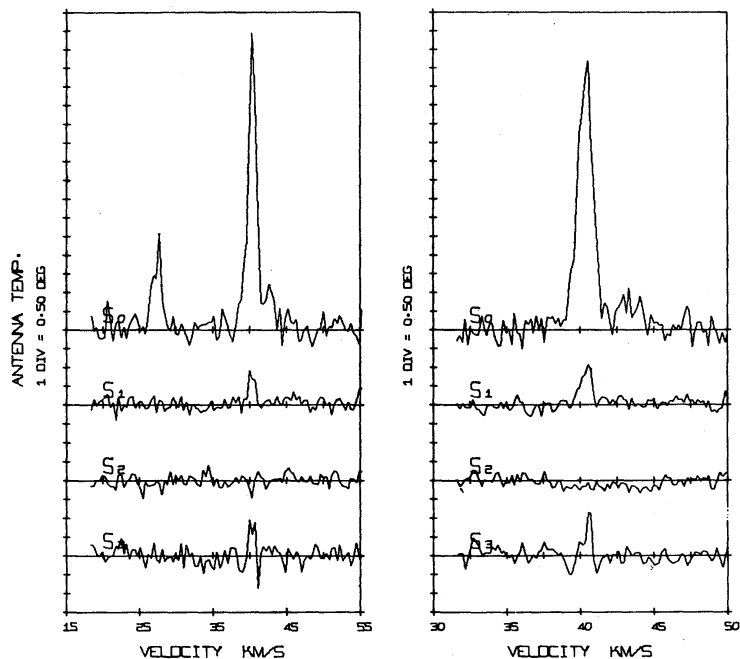


FIG. 6.—Source W43 at 1612 MHz, 1968 February (*left*) and May (*right*)

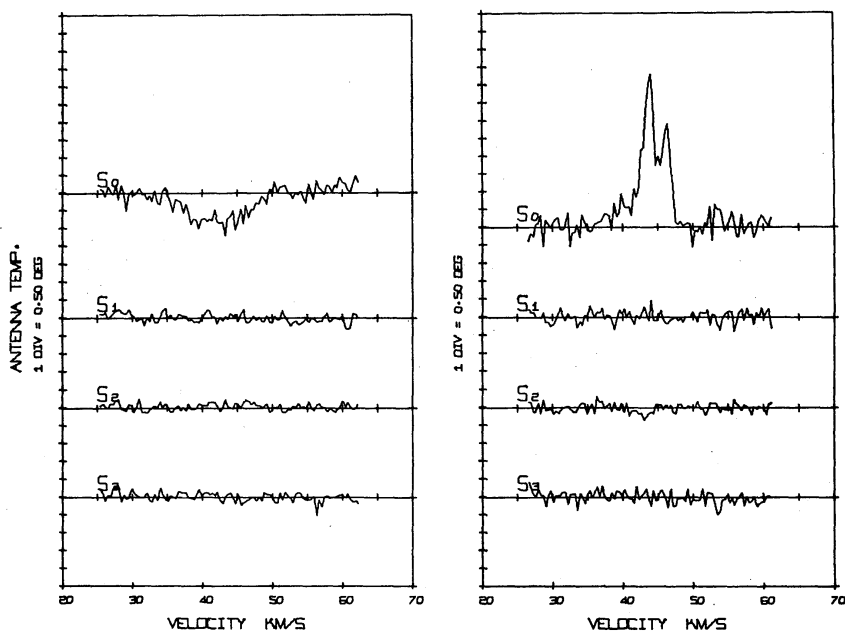


FIG. 7.—Satellite-line spectra of W44, 1968 February (*left*, 1612 MHz; *right*, 1720 MHz)

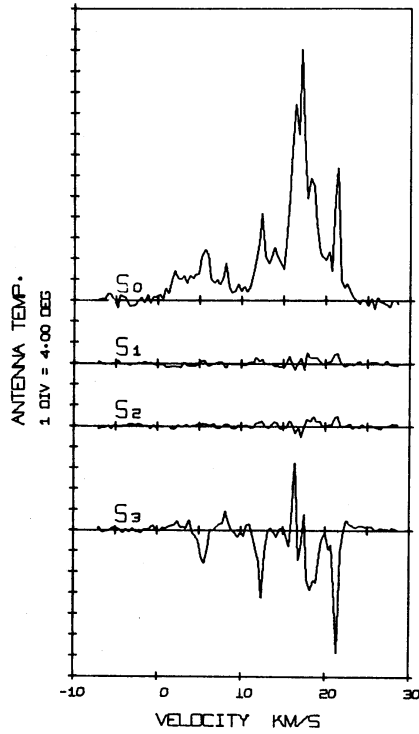


FIG. 8.—Source W49 at 1665 MHz 1968 May 6

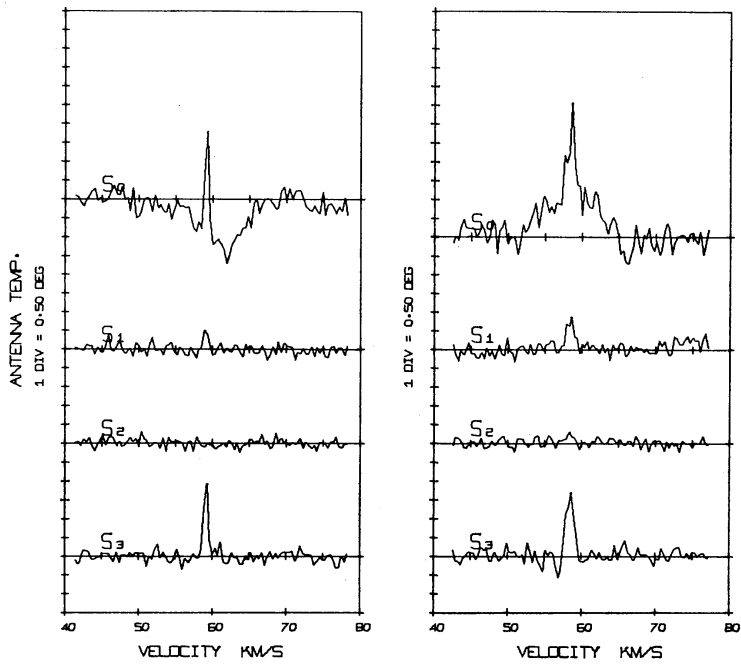


FIG. 9.—Satellite-line spectra of W51, 1968 February (*left*, 1612 MHz; *right*, 1720 MHz) near  $+60$  km sec $^{-1}$ .

There is a superposed emission consisting of several narrow highly polarized features. It is noteworthy that these have the same velocity and polarization at 1612 MHz as at 1720 MHz.

The powerful supernova remnant Cas A was the first source in which OH absorption was found. It has a sharp doublet of absorption due to the Orion arm and a group of four features due to the Perseus arm. The Orion-arm feature at 0 km sec<sup>-1</sup> is the strongest absorption line observed with the Hat Creek telescope. Our intention was to set as low a bound as possible upon the polarization and to use this feature as a check on instrumental bias. The model-fitting program, when applied to the results shown in Figure 11, gave an upper bound of 2 percent polarization for the stronger feature.

NGC 6334 is a nearby emission nebula at a distance of 1.14 kpc (Dieter 1967) in the direction of the galactic center. It has been studied with great care by Weaver *et al.*

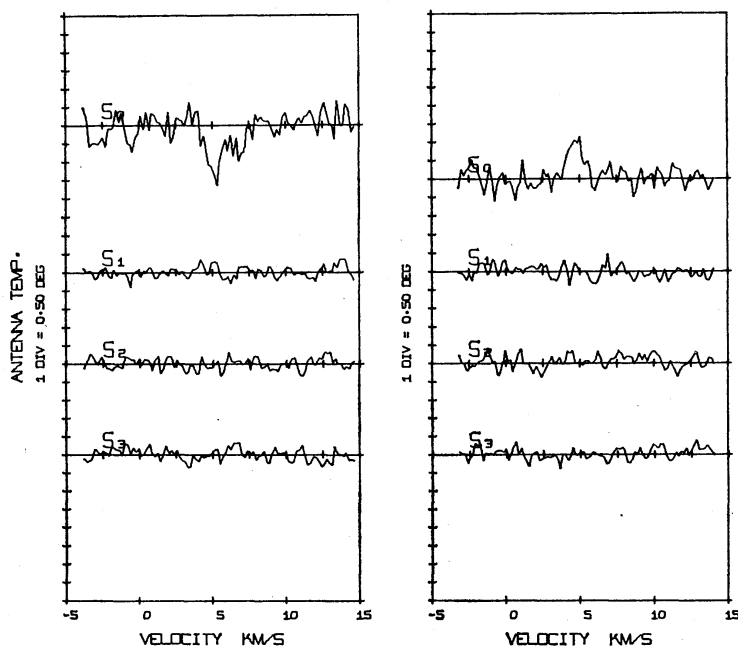


FIG. 10.—Satellite-line spectra of W51, 1968 May (*left*, 1612 MHz; *right*, 1720 MHz) near +5 km sec<sup>-1</sup>.

(1968) and by Ball and Meeks (1968), since the main-line OH emission has been found to vary with time. We observed it at a position midway between the two sources, on May 10, 15, and 23, but no significant variations were found. The spectra are not given because they cannot be compared in detail with those of other observers, for the reasons discussed by Ball and Meeks (1968).

The source S110 is a dark cloud at  $l = 168^{\circ}74$ ,  $b = 15^{\circ}50$ , in which Heiles (1968) has discovered “normal” OH emission. Our measurements showed no polarization, from which we conclude that the emission is less than 10 percent polarized.

### III. TIME VARIATIONS

Time variations in the main-line emission from NGC 6334 were discovered by Dieter (Weaver *et al.* 1968), and have been confirmed by Ball and Meeks (1968). Furthermore, a slow variation in the 1720-MHz emission from the source W49 has recently been reported by Zuckerman *et al.* (1968). The striking variations we have observed in W33 and, to a lesser degree, in W3 suggest that this extraordinary phenomenon may be characteristic of certain OH sources. In view of the importance of W33 observations, we have re-

examined these observations with great care. The nine individual sequences taken on February 15, 16, and 18 agree within the experimental error. Similarly, the eight sequences from May 11 to 14 agree, as do the four sequences for May 24. There may be a marginal difference between the average spectra for May 11 and 12, and for May 13 and 14. Various spurious effects which might cause an apparent time variation have been discussed in some detail by the groups studying NGC 6334. After careful examination of all such factors we believe that the observed variation in W33 is a property of the source for the following reasons.

a) The possibility that the variation might be due to variation in the receiver was

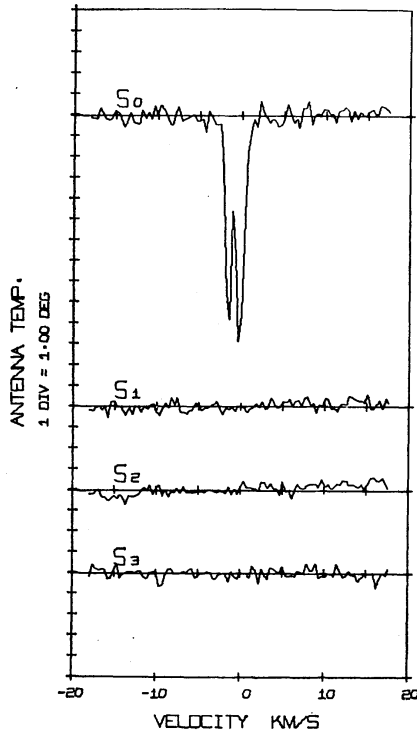


FIG. 11.—Cas A at 1667 MHz, 1968 February

ruled out by programming the observations so that a given Doppler velocity would be received in several independent channels of the receiver (see later discussion). Furthermore, the observations were alternated with observations of other sources.

b) Several features remained constant with time, and the two features which vary most obviously do not appear to be correlated in any way.

c) If the features are spatially separated, then there is a difference in the Doppler correction for the Earth's motion for different features, and this can produce an apparent variation between observations taken at significantly different times of the year. However, some of our variations appeared within days.

d) If the source is a complex of spatially separated features, it is possible to produce the observed variations with telescope pointing errors of a few minutes of arc. In our case this would require a constant error in all pointing done on May 14 compared with May 24. In fact, pointing errors are less than 1 minute of arc and are randomly distributed. Each of the spectra presented involves pointing on and off the source many times over a wide range of hour angles.

e) A slow decay of the strongest feature from 1968 April to June has also been observed by Turner (1968).

The apparent variation of W3 at 1665 MHz is not so clearly established, because it relies on observations with different telescopes. The clear implication is that NGC 6334 is not an isolated case, and that time variations are an intrinsic property of OH emission sources.

#### IV. CLASSIFICATION OF SOURCES

Despite the wide variation in their observable properties, the OH sources seem to fall into identifiable classes. Turner (1967) has divided the sources on the basis of their spectral properties. Ball and Staelin (1968) have made a similar division based on the nature of the nearest bright continuum source. The agreement between these two schemes is good, for almost all the sources in one of Turner's classes fall into the same class in Ball and Staelin's system. These results suggest a further development of this classification.

The classes proposed are: (a) the absorption sources; (b) the "normal" emission sources; (c) the main-line sources; (d) the strong satellite-line sources; and (e) the absorption-emission sources.

The absorption sources have been most thoroughly studied by Goss (1968). They seldom show the line ratios expected in an optically thin gas cloud in thermal equilibrium. Our observations suggest that they are unpolarized. Heiles (1968) has found "normal" emission from a number of interstellar dust clouds, which he interprets as thermal in nature. Our observations support this interpretation because we found no sign of polarization in the strongest of these sources. The "main-line sources" are the well-known sources, which show spectacular emission in one or both main lines. They are essentially the class I of Turner (1967) or class A of Ball and Staelin (1968).

Strong satellite-line emission was first observed by Goss (1968) in his absorption-line survey. There are few previous observations with high-frequency resolution or polarization measurement. The spectra are simpler than those of the main-line sources, showing only one or two obvious features in the total power spectrum. The emission appears in only one of the satellite lines in a given source, but has no obvious preference for either transition. These emission features tend to be broader and more weakly polarized than main-line features. The polarization has usually a complex structure with alternating right- and left-circular components in what is apparently a single feature. The satellite-line emission seems to be associated with nonthermal sources, and in the case of the Cygnus NML object with infrared emission (Wilson and Barrett 1968).

The absorption-emission sources show features only in the satellite lines, one transition being in emission and the other in absorption. The features tend to be much broader and weaker than those in the main-line sources, and they appear to be unpolarized. They are not clearly associated with any continuum source, but are more likely to show up in the spectra of a nonthermal source than in an H II region. They seem to be interstellar H I clouds well removed from continuum sources.

The features listed in Table 2 are classified according to this scheme in the last column of the table.

One of our initial objectives in this observation program was to obtain statistics on the distribution of the polarization parameters. This has not been possible because at this time observational selection still plays a major role in determining the "apparent" properties of the OH sources. Evidence suggests that there are several mechanisms involved in the OH emission process, and that we are not observing sources in all classes an equal number of times. For these reasons we have attempted to place the observed sources in "classes," but have not prepared statistics for the observations as a whole.

#### V. TELESCOPE AND RECEIVER

With the polarimeter feed the 85-foot Hat Creek dish is substantially underilluminated. We measured *E*-plane and *H*-plane beam widths of  $35.7 \pm 0.5$  and  $31.8 \pm 0.5$ ,

respectively. The pointing of the telescope has been discussed by Welch, Thornton, and Lohman (1966), who found residual errors with a standard deviation of about 0.4. Conversions between measured antenna temperature and flux can be based on our value of 15.5° K for Virgo A, which we assume to be a point source with a flux of 180 flux units at 1665 MHz. Hence, for a point source, 1° K corresponds to  $5.8 \pm 0.5$  f.u. This value is consistent with a comparison between our spectra for W49 at 1665 MHz and those of Ball and Meeks (1968).

The receiver used was a room-temperature parametric amplifier which was Dicke-switched, either between nominally orthogonal polarizations or against a sky-horn reference. The radiometer was followed by a 100-channel filter-bank spectrometer which consists of two independent 50-channel banks, and is discussed in detail by Weaver *et al.* (1968). The system noise temperature, including the polarimeter and the ferrite switch, was about 210° K. The channel bandwidth used for all the observations was 2 kHz. The February observations were made with the two 50-channel filter banks in series, giving a total width of 200 kHz. Most of the May observations were made with the two banks interlaced, giving two samples per channel width over a total width of 100 kHz. The spectrometer output was digitally integrated for a fixed period, and the results were punched on cards for later computer reduction.

#### VI. MEASUREMENTS OF POLARIZATION

The polarimeter is designed to take advantage of the Dicke-switched radiometer, which is particularly suitable for the difference measurements that define the Stokes parameters. It receives two orthogonal linear polarizations, which are combined in a system of transfer switches and hybrid junctions. Appropriate settings of these transfer switches yield orthogonal circular polarizations, or various pairs of orthogonal linear polarizations, at the two input ports of the radiometer switch. Considerable redundancy is provided in the range of polarization settings in order to check the significance of the results. It is important to note that the accuracy of measurement does not assume that these polarizations are exactly orthogonal or perfect in any way, because the polarizations actually used are determined by direct calibration. A least-squares data-reduction procedure is then used to eliminate the instrumental bias.

It is convenient to consider the radiation to be measured as a four vector  $\mathbf{S}$ , whose components are the four Stokes parameters. An estimate of  $\mathbf{S}$  is obtained as follows. Let  $\boldsymbol{\theta}$  be a vector whose components consist of the received power for the various antenna polarizations used. Thus we can write

$$\boldsymbol{\theta} = A\mathbf{S} + \boldsymbol{\varepsilon},$$

where  $\boldsymbol{\theta}$  has dimension  $m \geq 4$ ,  $A$  is the calibration matrix, whose elements represent the measured polarization characteristics of the antenna,  $\mathbf{S}$  is the source vector we are trying to measure, and  $\boldsymbol{\varepsilon}$  is the error vector, for which the elements are independent, normally distributed, random variables with zero means. There is a maximum-likelihood estimator ( $\mathbf{S}^*$ ) for  $\mathbf{S}$  which is also minimum variance and unbiased. It is known to be (Mood and Graybill 1963)

$$\mathbf{S}^* = (A^t C^{-1} A)^{-1} A^t C^{-1} \boldsymbol{\theta},$$

where  $\sigma^2 C$  is the diagonal covariance matrix for  $\boldsymbol{\varepsilon}$ , such that  $C$  is a weighting factor which would be the identity matrix if all the measurements had the same variance  $\sigma$ , and  $A^t$  is the transpose of  $A$ .

It is clear that when there is exactly four measurements—i.e., no redundancy— $A$  is square and nonsingular. The solution then simplifies to  $\mathbf{S}^* = A^{-1} \boldsymbol{\theta}$ .

The covariance matrix of  $\mathbf{S}^*$  is  $\sigma^2 (A^t C^{-1} A)^{-1}$ , which depends on the set of measurements chosen through  $A$ , and on the accuracy of each measurement through  $C$ . It is desirable that the set of observations be chosen so that  $\text{cov}(\mathbf{S}^*)$  is a diagonal matrix. Other-

wise there is a correlation between the estimates of the various Stokes parameters, which makes their interpretation deceptive.

If there are more than four independent measurements, we can also estimate  $\sigma^2$ . The minimum variance unbiased estimate is

$$(\sigma^2)^* = \frac{1}{m-4} (\theta - AS)^t C^{-1} (\theta - AS).$$

Thus the redundancy produces a useful error estimate without reducing the efficiency. Any correlation between  $(\sigma^2)^*$  and  $S_0$  indicates either that there is an error in the calibration matrix  $A$  or that the system gain has changed during the observations.

The matrix  $A$  was determined by measuring the polarization transmitted from the polarimeter (for a given setting of the switches) to the center of the dish. The precision of these measurements was about 0.1 percent in power. It turns out, however, that the addition to purely right-handed circular polarization of 0.1 percent in power of left-handed circular polarization produces an axial ratio (in the polarization ellipse) of 0.87. This was the effect of a 13 percent error in  $S_3$  on the measurement of circular polarization in the presence of strong linear polarization. However, this can be compensated by averaging the results for  $S_3$  taken with orthogonal position angles of the polarimeter (see Appendix).

#### VII. OBSERVATIONAL PROCEDURE

The observational procedure consisted of a sequence of 10-minute observations using various linear and circular polarizations plus a calibration and an observation of a reference region. The observations were chosen to give the following covariance matrix for  $S$ :

$$\text{cov}(S) = \begin{vmatrix} 3 & 0 & 0 & 0 \\ 0 & 1 & 0 & 0 \\ 0 & 0 & 1 & 0 \\ 0 & 0 & 0 & 1 \end{vmatrix}$$

The spectra were fitted to a model consisting of a superposition of uniformly polarized, independent features with Gaussian profiles. The least-squares fitting of such a model to the four estimated spectra is a nonlinear problem with a nonunique solution. The problem has been discussed by many authors for single spectra (Kaper *et al.* 1966; von Hoerner 1966), and computer programs are available. We have used a program developed by N. H. Dieter in an iterative manner; it is not certain to converge, but if it does, the solution is correct. The restriction to uniformly polarized features implies that the center and width of each feature must be the same in all four spectra. The nonuniqueness is removed by taking the simplest model that includes the obvious features, converges, and leaves a reasonable root mean square error.

We are indebted to the staff of the Hat Creek Observatory and to the Director, Dr. Weaver, for their assistance in this work.

#### APPENDIX

The nonlinear coupling of linear polarization into circular measurements may be analyzed conveniently if the coherency matrix  $J$  is used. It is defined by

$$J_{rr} = \langle E_r^* E_r \rangle = \frac{1}{2}(S_0 + S_3),$$

$$J_{ll} = \langle E_l^* E_l \rangle = \frac{1}{2}(S_0 - S_3),$$

$$J_{rl} = \langle E_r^* E_l \rangle = \frac{1}{2}(S_1 + iS_2),$$

$$J = \begin{pmatrix} J_{rr} & J_{rl} \\ J_{lr} & J_{ll} \end{pmatrix}.$$

When the polarimeter is set to receive nominally right-circular polarization, it would transmit a normalized field,

$$E = e_r \sqrt{1 - |\epsilon_r|^2} + e_l \epsilon_r,$$

where  $e_r$  and  $e_l$  are the unit vectors for right- and left- circular polarization, respectively, and  $\epsilon_r$  is a complex number specifying the amplitude and phase of the left-circular component, relative to the right-circular component. Its coherency matrix is then

$$P = \begin{pmatrix} 1 - |\epsilon_r|^2 & \epsilon_r^* \sqrt{1 - |\epsilon_r|^2} \\ \epsilon_r \sqrt{1 - |\epsilon_r|^2} & |\epsilon_r|^2 \end{pmatrix}.$$

The response to a wave with coherency matrix  $J$  is the trace of  $JP$ . Thus

$$T(R) = (1 - |\epsilon_r|^2)J_{rr} + |\epsilon_r|^2 J_{ll} + 2\sqrt{1 - |\epsilon_r|^2} \text{Real}(J_{rl}\epsilon_r^*).$$

The first-order error (due to the fact that  $\epsilon_r$  is not zero) is the last term. A rotation of  $90^\circ$  in position angle is equivalent to a phase change of  $180^\circ$  in  $e_l$  with  $e_r$  fixed. Hence,

$$\frac{1}{2}[T(R)_0 + T(R)_{90}] = (1 - |\epsilon_r|^2)J_{rr} + |\epsilon_r|^2 J_{ll}.$$

This eliminates the first-order error. The effective gain,  $(1 - |\epsilon_r|^2)$  is never less than 98 percent and can be accurately calibrated.

#### REFERENCES

- Ball, J. A., and Meeks, M. L. 1968, *Ap. J.*, **153**, 577.  
 Ball, J. A., and Staelin, D. H. 1968, *Ap. J. (Letters)*, **153**, L41.  
 Coles, W. A., Rumsey, V. H., and Welch, W. J. *Ap. J. (Letters)*, **154**, L61.  
 Dieter, N. H. 1967, *Ap. J.*, **150**, 435.  
 Goss, W. M. 1968, *Ap. J. Suppl.*, **137**, 131.  
 Heiles, C. E. 1968, *Ap. J.*, **151**, 919.  
 Hollinger, J. P., and Hobbs, R. W. 1966, *Science*, **153**, 1633.  
 Kaper, H. G., Smits, D. W., Schwarz, U., Takakubo, K., and van Woerden, H. 1966, *B.A.N.*, **18**, 465.  
 Kraus, J. D. 1966, *Radio Astronomy* (New York: McGraw-Hill Book Co.).  
 Meeks, M. L., Ball, J. A., Carter, J. C., and Ingalls, R. P. 1966, *Science*, **153**, 978.  
 Mezger, P. G., and Henderson, A. P. 1967, *Ap. J.*, **147**, 471.  
 Mezger, P. G., and Höglund, B. 1967, *Ap. J.*, **147**, 490.  
 Mood, A. M., and Graybill, F. A., 1963, *Introduction to the Theory of Statistics* (2d ed.; New York: McGraw-Hill Book Co.), pp. 343-350.  
 Palmer, P., and Zuckerman, B. 1967, *Ap. J.*, **148**, 727.  
 Turner, B. E. 1968, A.A.S. meeting, Victoria, B.C.  
 von Hoerner, S. 1967, *Ap. J.*, **147**, 467.  
 Weaver, H. 1968, private communication.  
 Weaver, H., Dieter, N. H., and Williams, D. R. W. 1968, *Ap. J. Suppl.*, **146**, 219.  
 Welch, W. J., Thornton, D. D., and Lohman, R. 1966, *Ap. J.*, **146**, 799.  
 Wilson, W. J., and Barrett, A. H. 1968, A.A.S. meeting, Victoria, B.C.  
 Zuckerman, B., Penfield, H., Lilley, A. E., Palmer, P., Dickinson, D. F., and Ball, J. A. 1968, A.A.S. meeting, Victoria, B.C.

